FEBS Letters 585 (2011) 791–796

journal homepage: www.FEBSLetters.org

Mice lacking Ran binding protein 1 are viable and show male infertility

Masahiro Nagai [a,b], Tetsuji Moriyama [a], Rashid Mehmood [a], Keizo Tokuhiro [c], Masahito Ikawa [d], Masaru Okabe [d], Hiromitsu Tanaka [c], Yoshihiro Yoneda [a,b,e,*]

[a] Biomolecular Dynamics Laboratory, Department of Frontier Biosciences, Graduate School of Frontier Biosciences, Osaka University, 1-3 Yamada-oka, Suita, Osaka 565-0871, Japan
[b] Department of Biochemistry, Graduate School of Medicine, Osaka University, 2-2 Yamada-oka, Suita, Osaka 565-0871, Japan
[c] TANAKA Project, Center for Advanced Science and Innovation, Osaka University, 3-1 Yamada-oka, Suita, Osaka 565-0871, Japan
[d] Research Institute for Microbial Diseases, Osaka University, 3-1 Yamada-oka, Suita, Osaka 565-0871, Japan
[e] JST, CREST, Osaka University, 1-3 Yamada-oka, Suita, Osaka 565-0871, Japan

ARTICLE INFO

Article history:
Received 12 October 2010
Revised 31 January 2011
Accepted 1 February 2011

Edited by Ulrike Kutay

Keywords:
Ran binding protein 1 (RanBP1)
Ran binding protein 2 (RanBP2)
RanGTPase activity

ABSTRACT

The small GTPase Ran plays important roles in multiple aspects of cellular function. Maximal RanGAP activity is achieved with the aid of RanBP1 and/or presumably of RanBP2. Here, we show that RanBP1-knockout mice are unexpectedly viable, and exhibit male infertility due to a spermatogenesis arrest, presumably caused by down-regulation of RanBP2 during spermatogenesis. Indeed, siRNA-mediated depletion of RanBP2 caused severe cell death only in RanBP1-deficient MEFs, indicating that simultaneous depletion of RanBP1 and RanBP2 severely affects normal cell viability. Collectively, we conclude that the dramatic decrease in "RanBP" activity impairs germ cell viability and affects spermatogenesis decisively in RanBP1-knockout mice.

1. Introduction

Small GTPase Ran [1] plays important roles not only in fundamental cellular activities (nucleo-cytoplasmic transport, mitotic spindle assembly, and nuclear envelope formation [2–8]), but also in tissue activities such as nerve cell response to axon injury [9]. The asymmetric distribution of RanGTP in the nucleus and RanGDP in the cytoplasm is regulated by nuclear RCC1 (RanGEF) [1] and cytoplasmic RanGAP (=GTPase activating protein) [10]. In addition, however, biochemical analyses have shown that the activity of RanGAP is achieved with the aid of a Ran binding protein, RanBP1 [11]. Cytoplasmic RanBP1 serves as a crucial cofactor for stimulating RanGAP activity [12] by dissociating RanGTP-containing complexes that exit from the nucleus [13] (Fig. S1). Although *Caenorhabditis elegans* and *Drosophila melanogaster* do not have direct homologues of *RanBP1* [6], *Saccharomyces cerevisiae* possesses a *RanBP1* homologue (*Yrb1*) as an essential gene. Temperature-sensitive mutants of *Yrb1* show deficiency in nuclear import and poly A^+ RNA export activity [14,15]. Among identified Ran binding proteins in mammals, only Ran binding protein 2 (RanBP2 [16]; also called Nup358, a giant nucleoporin) contains RanBP1-like domains that show high affinity to Ran, so RanBP2 is biochemically predicted to be the sole functional substitute for RanBP1 [2–8]. In addition, it has recently been demonstrated that the null allele of the mouse *RanBP2* gene causes embryonic lethality [17,18]. Although the functions of RanBP1 have been well investigated at the cellular level [2–8,19,20], its roles at the level of the organism remain to be understood.

2. Materials and methods

2.1. Cell culture

Mouse embryonic fibroblasts (=MEFs) were cultured in DMEM supplemented with 10% FBS, at 37 °C, 5% CO_2.

2.2. Preparation of tissue and cell lysates

Fresh tissues obtained from 12-week old male mice or MEFs were lysed with buffer (4 M Urea, 50 mM Tris–HCl (pH 8.0), 150 mM NaCl, 0.1% SDS, 1 mM EDTA with 10 μg/ml each of leupeptin, aprotinin, and pepstatin), and after centrifugation at 15 000 rpm for 10 min, the supernatant was used.

2.3. Generation of RanBP1-knockout mice

The targeting vector was constructed with the use of pMulti-ND 1.0 vector (a kind gift from Dr. J. Takeda and T. Ijiri) containing the

* Corresponding author at: Biomolecular Dynamics Laboratory, Department of Frontier Biosciences, Graduate School of Frontier Biosciences, Osaka University, 1-3 Yamada-oka, Suita Osaka 565-0871, Japan. Fax: +81 6 6879 4609.
E-mail address: yyoneda@anat3.med.osaka-u.ac.jp (Y. Yoneda).

0014-5793/$36.00
doi:10.1016/j.febslet.2011.02.002

Neo-resistance gene (*neo*^{r}) as a positive selection marker and diphtheria toxin A chain (DT) as a negative selection marker. The 5′ short arm spanned exon 1 and the 3′ long arm included exon 3 and exon 4. The short and long arms were cloned into the pMulti-ND-1.0 plasmid. The targeting construct was electroporated into D3 embryonic stem (ES) cells. *RanBP1* mutant cells obtained by homologous recombination were identified by PCR and Southern blot analysis. Targeted ES cell clones were microinjected into C57BL/6 blastocists to generate chimeric mice. Chimeras were then mated to C57BL/6 mice for germline transmission.

2.4. Southern blot and PCR analysis

Southern blot hybridization was used to confirm short-arm recombination in the embryonic stem cells using standard protocols. Specifically, targeted clones were identified using a 5′ external probe, which detects the change of a 9.6 kb WT BamHI/NdeI fragment to a novel 3.5 kb BamHI/NdeI fragment. To confirm long-arm recombination, long arm PCR was performed using LA-Taq^{TM} (TaKaRa) according to the manufacturer's instructions, with the shared primer (see Fig. 1A) **1**(5′-GTTTCTCCTCAGACTTCTCTTCAGCCTCC-3′) and three pairs of primers. **2**(5′-TCTGTTGTGCCCAGTCATAGCCGAATAGCC-3′) to amplify a ~8 kb PCR product, **3**(5′-TTGGCGCCTACC GGTGGATGTGGAATGTGTG-3′) to amplify a ~7.6 kb PCR product, **4**(5′-GCTACTTCCATTTGTCACGTCCTGCACGACG-3′) to amplify a ~7.7 kb PCR product, respectively.

PCR products were resolved on 1% agarose gels.

2.5. Genotyping of the offspring was performed to detect the WT and mutant alleles

For genotyping PCR (see Fig. 1A), the shared primer (3) (5′-ACCCATTGATGTTTGAGTGTGTAGGAGTGTC-3′) was designed upstream of the deleted region. This primer can pair with WT allele-specific primer (2) (5′-CTCATCTGCATTCTCTGTGGAAGTATCATGG-3′) to amplify a ~300 bp PCR product or with the targeted allele-specific primer (1) (5′-GCCTTCTATCGCCTTCTTGACGAGTT CTTC -3′) in the *neo* cassette to amplify a ~430 bp fragment from the mutant allele. PCR was performed with rTaq^{TM} (TaKaRa) according to the manufacturer's instructions, and PCR products were resolved on 2% agarose gels.

2.6. Continuous breeding assay

(Male) 8-week old *RanBP1*$^{+/-}$ and $^{-/-}$ male mice were mated with two wild-type (=WT) female mice and the cumulative number of progeny was counted for the period indicated.

(Female) 8-week old *RanBP1*$^{+/-}$ and $^{-/-}$ female mice were mated with three RanBP1$^{+/-}$ male mice and the cumulative number of progeny was counted for the period indicated.

2.7. Histology of testis sections

Fresh mouse testis and epididymis were fixed in 10% formalin neutral buffer solution, embedded in paraffin. Sections (7 μm) were stained with Hematoxilin-Eosin (HE).

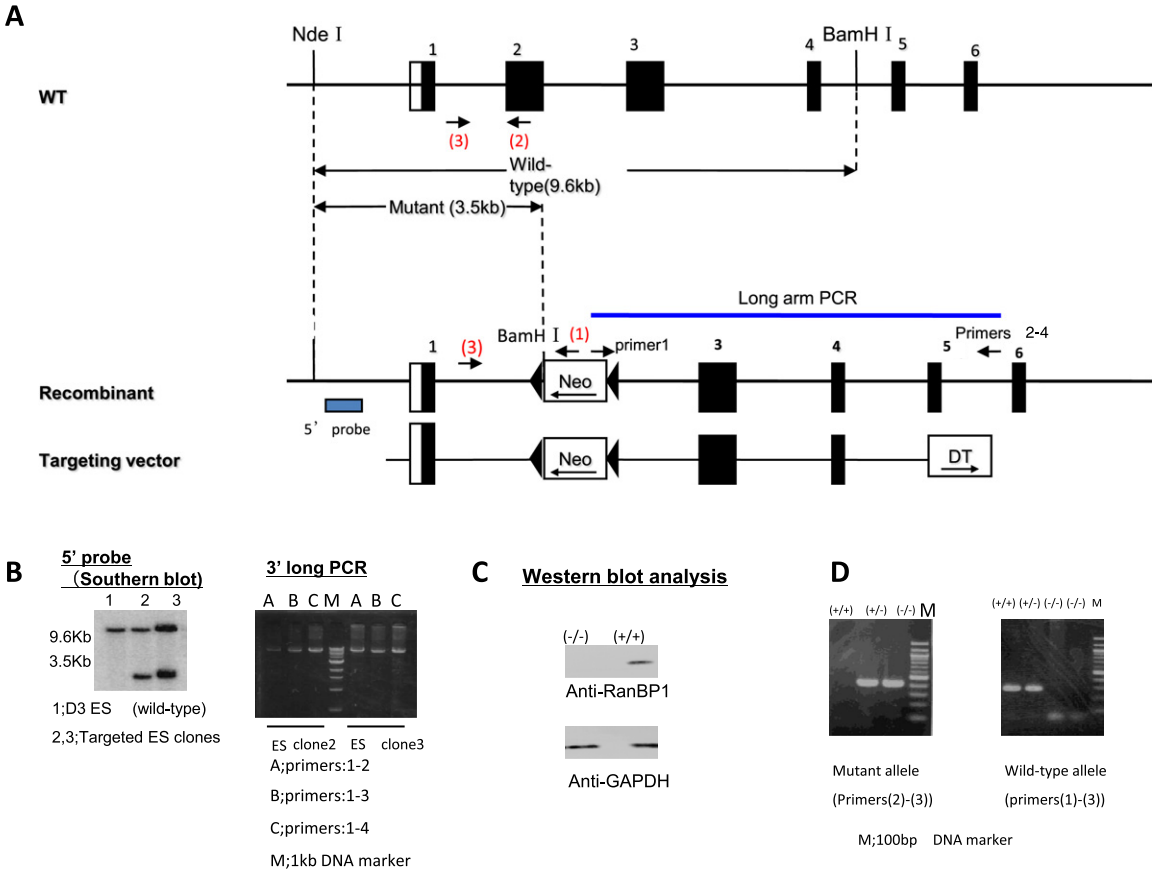

Fig. 1. Generation of RanBP1-knockout mice. (A) Genomic organization and targeting strategy for *RanBP1* gene disruption. (B) Southern blot analysis (5′ arm) and PCR-based analysis (3′ arm) of WT and *RanBP1*$^{+/-}$ ES cells. (C) Immunoblot of brain lysates from WT and *RanBP1*$^{-/-}$ mice (GAPDH as a loading control). (D) PCR-based genotyping of *RanBP1*$^{+/+}$, $^{+/-}$, and $^{-/-}$ mice.

2.8. In situ apoptosis detection

Testis sections (8 μm) of *RanBP1*$^{+/-}$ and *RanBP1*$^{-/-}$ male mice were assayed for in Situ TUNEL assay using in situ Apoptosis Detection Kit (TaKaRa).

2.9. Age-blot analysis

Testis from wild-type (WT) male mice of 1–5 weeks of age were lysed in RIPA buffer (10 mM Tris–HCl (pH 7.6), 0.15 M NaCl, 0.1% SDS, 0.1% sodium deoxycholate, 1% NP-40).

2.10. Antibodies

Ran (Sigma, ARAN1), RanBP1 (Santa Cruz, M-45), RanBP2 (Covance, mAb414 for immunoblot) (abcam for immnohistochemstry), RanGAP (Zymed Laboratories), RCC1 (Santa Cruz, N-19), Actin (Santa Cruz, C-11), GAPDH (Ambion, Cat#4300).

2.11. Proliferation and viability analyses of MEFs and procedures of small interfering RNA (=siRNA) treatment

For proliferation analysis, 1×10^4 MEFs (passage 3) were plated in triplicate on 12-well plates. The next day, MEFs were transfected with 15 nM siRNA-oligonucleotide against mouse RanBP2 (5′-CCAGUCACUUACAAUUAAATT-3′), and luciferase (5′-AGCUUCAUAAGGCGCAUGCTT-3′) using Lipofectamine™ RNAiMAX (Invitrogen). For proliferation analysis, trypsinized MEFs were counted at 1 to 4 days after transfection. For viability analysis, MEFs (96 h after transfection) were trypsinized, centrifuged, and the dead cell proportion was judged by trypan-blue staining.

2.12. Statistical analysis

The student's *t*-test (two-tailed) was used.

3. Results and discussion

3.1. RanBP1-knockout mice are viable

To know the functions of RanBP1 at the organism level, we first examined the expression levels of the RanBP1 protein in various mouse tissues. We found that RanBP1 was ubiquitously expressed in the tissues examined (Fig. S2). In order to elucidate in vivo roles of *RanBP1*, we next generated RanBP1-knockout mice utilizing mouse embryonic stem (ES) cells (Fig. 1). Surprisingly, against our expectation and in contrast to the case of RanBP2-knockout mice, *RanBP1*$^{-/-}$ mice were born alive, albeit at a lower frequency than would be expected from Mendel's Law (+/+: +/−: −/− = 1:1.91:0.25 (n = 360), on a mixed background including C57BL/6 and 129 alleles). Western-blot analysis of *RanBP1*$^{-/-}$ brain lysate confirmed the complete absence of RanBP1 protein (Fig. 1C), indicating that *RanBP1* is not necessarily essential in mice, unlike in budding yeast, although *RanBP1* apparently has some effects on mouse embryogenesis.

3.2. RanBP1-knockout mice show growth retardation and male infertility

However, we noticed that at birth, *RanBP1*$^{-/-}$ mice had small body size without any apparent morphological abnormalities. This body weight deficit became more pronounced as the mice aged. At the age of 12 weeks, *RanBP1*$^{-/-}$ mice showed ~32% body weight reduction, as compared to WT littermates (Fig. 2A and B). We also observed a few severe cases of *RanBP1*$^{-/-}$ mice that were 50–60% smaller than their WT littermates (Fig. 2C). Additionally, *RanBP1*$^{-/-}$ mice exhibited male-specific infertility (Fig. 3A and B). Indeed, when adult *RanBP1*$^{-/-}$ male mice were mated to WT female mice (C57BL/6), none of the female mice conceived (Fig. 3A), although these mice copulated normally, as evidenced by the formation of vaginal plugs (data not shown). On the other hand, *RanBP1*$^{-/-}$ female mice were not infertility (Fig. 3B). Therefore, in this study, we focused on examination of testis development in the *RanBP1*$^{-/-}$ mice.

3.3. Male infertility of RanBP1-knockout mice appears to be caused by the decrease of RanBP2 at the stage of elongating spermatids in the context of RanBP1-deficiency

Mouse spermatogenesis is a complex process that takes ~35 days after birth. The process involves three major events: proliferation of spermatogonial cells, meiotic division of spermatocytes, and differentiation from haploid spermatids to mature sperm [21,22]. Detailed histological analysis revealed that the germ cells of *RanBP1*$^{-/-}$ male mice completed meiosis and formed round spermatids but gradually ceased to differentiate, resulting in impairment of spermatogenesis around the time of spermatid elongation; only few elongated spermatids were observed (Fig. 3C–E), and the epididymides of *RanBP1*$^{-/-}$ mouse testis lacked mature sperm (Fig. 3F and G). Furthermore, TUNEL assay revealed that there were 5.54 ± 0.86 (mean ± S.E.) apoptotic cells/tubule in the testis of *RanBP1*$^{-/-}$ mice, as compared to and 1.30 ± 0.28 in *RanBP1*$^{+/-}$ mice (Fig. S3A). In *RanBP1*$^{-/-}$ mice, round spermatids or spermatocytes were detected in seminiferous tubules, and some sperm nuclei in the tubule were detected near the tubule walls, but not in the center (Fig. S3B and C).

Next, in order to understand how the decisive spermatogenesis defect occurred at the stage of spermatid formation in *RanBP1*$^{-/-}$ testis, we analyzed the expression patterns of Ran and RanGTPase partners (RanBP1, RanBP2, RanGAP, and RCC1) during mouse spermatogenesis using testis lysates from 1 to 5 week old WT mice. We found that the expression levels of RanBP1, RanGAP, RCC1, and Ran did not change significantly during spermatogenesis (Fig. 4A–F). In contrast, RanBP2 protein showed a dramatic decrease at the stage of spermatid elongation (corresponding to 4 weeks old) (Fig. 4C), just when *RanBP1*$^{-/-}$ germ cells ceased to differentiate. The expression pattern of RanBP2 was also confirmed by immunohistochemistry in WT testis sections (Fig. S4).

Since it has been established biochemically that both RanBP1 and RanBP2 function as positive regulators for RanGAP activity, the depletion of both factors should cause a severe defect in RanGTPase activity, damaging diverse cellular functions mediated by Ran. Therefore, it seems possible that the decisive defect in spermatogenesis observed in *RanBP1*$^{-/-}$ testis is caused by perturbation of RanGTPase activity in germ cells when RanBP2 is downregulated in the context of RanBP1-deficiency.

3.4. RanBP2-depletion suppresses cell viability in *RanBP1*$^{-/-}$MEFs

To explore this possibility and owing to technical difficulties in culturing male germ cells, we established *RanBP1*$^{-/-}$ MEFs and introduced siRNA oligo duplexes against *RanBP2* to mimic the situation of spermatids in *RanBP1*$^{-/-}$ testis (Fig. 5A). As shown in Fig. 5B, at 48 h after siRNA treatment, RanBP2-specific siRNA-treated WT MEFs showed comparable proliferation as compared to control siRNA-treated WT MEFs. In contrast, RanBP2-specific siRNA-treated *RanBP1*$^{-/-}$ MEFs showed decreased proliferation as compared to control siRNA-treated *RanBP1*$^{-/-}$ MEFs. In addition, 72 and 96 h after siRNA treatment, RanBP2-siRNA-treated *RanBP1*$^{-/-}$ MEFs showed a dramatic decrease in proliferation as

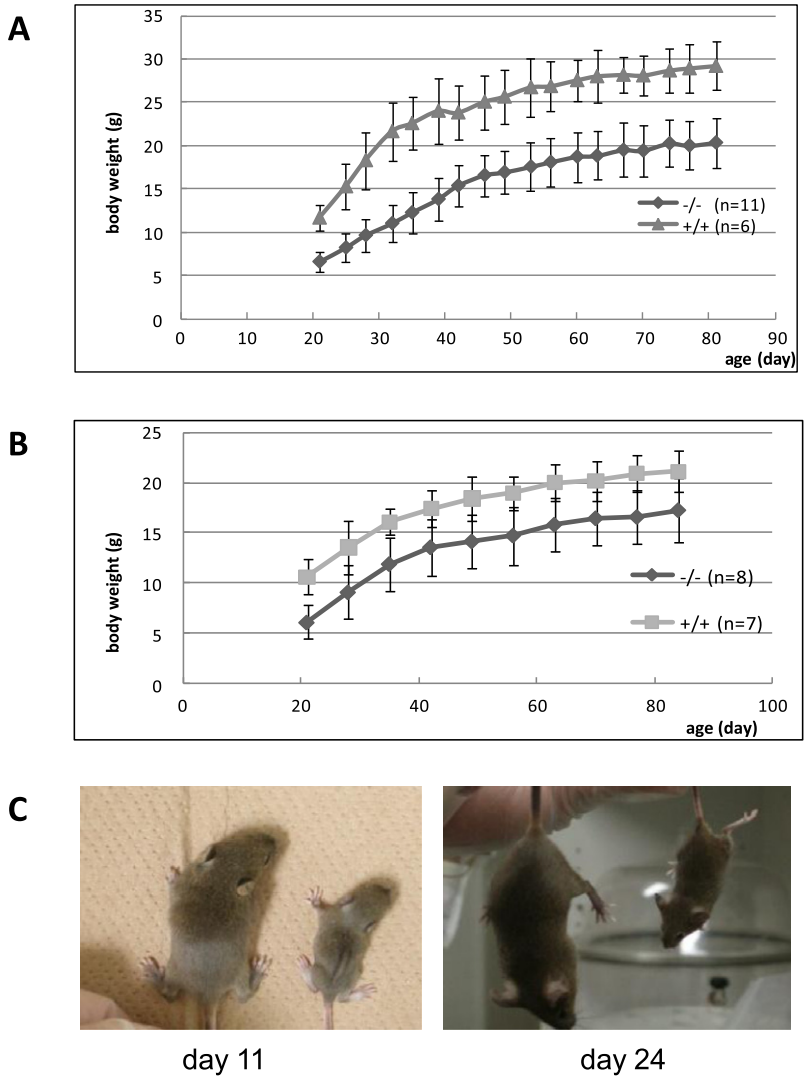

Fig. 2. RanBP1-knockout mice are viable. (A and B) Growth curves of male (A) and female (B) mice (means ± S.D.). (C) Appearance of *RanBP1*$^{+/+}$ (left) and *RanBP1*$^{-/-}$ (right) male littermates (postnatal day 11 and day 24).

compared to control-siRNA-treated *RanBP1*$^{-/-}$ MEFs, while proliferation of RanBP2-specific siRNA-treated WT MEFs was decreased to a lesser extent (Fig. 5B). Furthermore, we found that cell viability was significantly decreased in RanBP2-specific siRNA-treated *RanBP1*$^{-/-}$ MEFs compared with RanBP2-specific siRNA-treated WT MEFs (86.2% vs. 17.4%, $P = 1.36 \times 10^{-5}$) (Fig. 5C). These results indicate that RanBP2-depletion in the context of RanBP1-deficiency strongly suppresses cell proliferation and viability, while down-regulation of RanBP2 alone affects them to a lesser extent.

Based on these experiments, in RanBP1-knockout mice, it is reasonable to suppose that the decisive impairment of spermatogenesis observed at the stage of spermatid elongation is caused by the loss of "RanBP" activity due to the simultaneous depletion of RanBP1 and RanBP2, while the apoptotic signals at the stage of spermatocyte would be the influence of RanBP1-deficiency alone, and that the signals near the tubule walls may show the degraded products of sperm nuclei that were phagocytosed by Sertoli cells as in the case of meichroacidin (MCA)-knockout mice [23].

4. Discussion

This study showed that RanBP1-knockout mice are viable and, during spermatogenesis, the proliferation of spermatogonial cells and the meiotic division of spermatocytes do not necessarily require RanBP1, presumably because of functional complementation by RanBP2. However, we also observed that RanBP1-knockout mice are born at a lower ratio than 25%, and exhibit growth retardation after birth. These data indicate that RanBP1 has some function(s) that are not completely compensated by RanBP2.

In contrast to the results reported herein, previous studies have reported that RanBP2-knockout mice display an embryonic lethal phenotype [17,18]. These results indicate that RanBP1 cannot compensate for the function of RanBP2 during embryogenesis, suggesting that RanBP2 is more critical than RanBP1 for the RanGTPase activity and/or that RanBP2 possesses independent roles. RanBP2 locates at the cytoplasmic rim of the nuclear pore complex (=NPC), whereas RanBP1 is dispersed in the cytoplasm [2–8], it is therefore possible that RanBP2 first captures outgoing RanGTP-containing export complexes and SUMO (=small ubiquitin-like modifier)-modified RanGAP that is associated with RanBP2 immediately mediates GTP hydrolysis by Ran to dissociate the export complex, while RanBP1 may function as a "back-up" factor for this process.

The human *RanBP1* gene is located at chromosome 22q11.2. Patients of DiGeorge syndrome (DGS), a frequent hereditary disease that exhibits a wide range of symptoms, commonly lack the 22q11.2 region in a haplo-insufficient manner [24]. Although

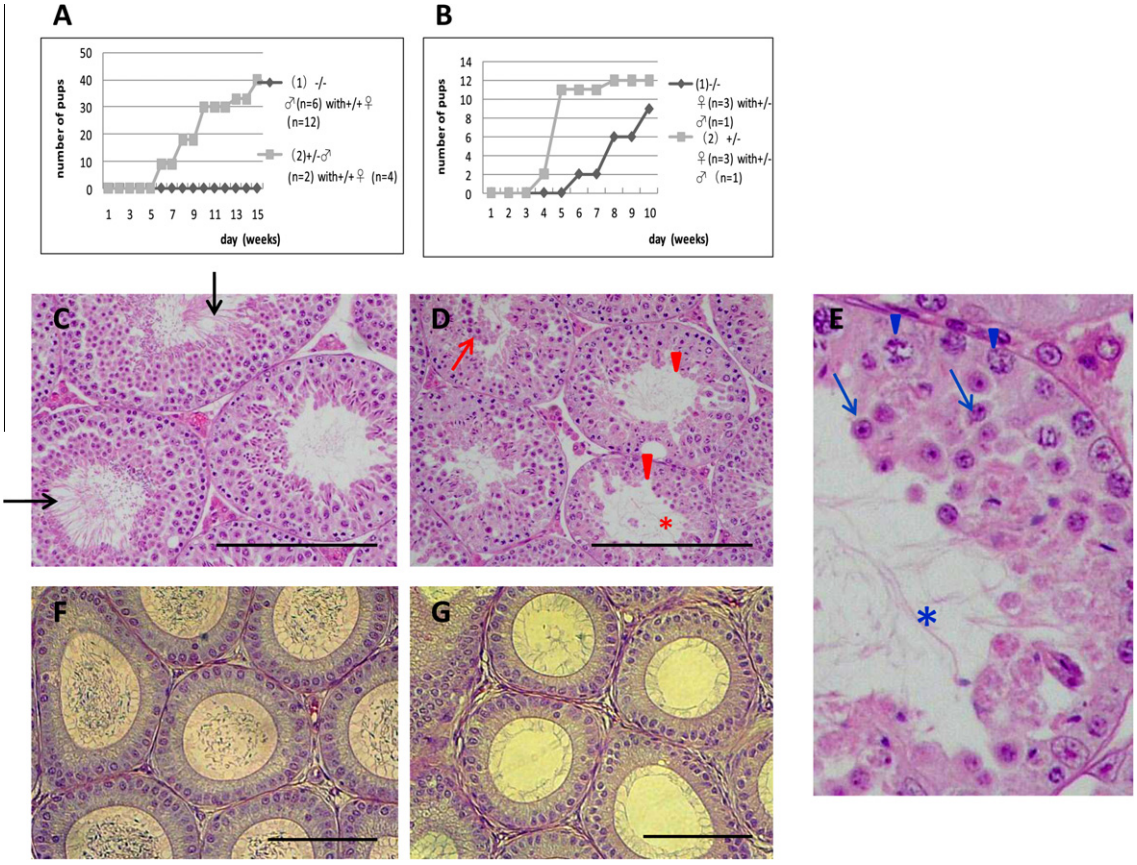

Fig. 3. Male infertility of RanBP1-knockout mice. (A and B) Continuous breeding assay starting at 8 weeks of age, showing cumulative number of progeny (male (A) and female (B)). (C and D) Haematoxylin and eosin (HE) staining of seminiferous tubules from *RanBP1*$^{+/+}$ (C) and *RanBP1*$^{-/-}$ (D) mice (scale bar 100 μm). The number of round spermatids decreased, and elongated spermatids were rare in the center of seminiferous tubules (Red arrow heads). The red arrow indicates spermatocytes of seminiferous tubules. (E) Higher magnification images of the locus indicated by a red star in seminiferous tubules from *RanBP1*$^{-/-}$ testis. Elongated spermatids were rare in the center of seminiferous tubules (Blue star); tails and a few immature heads of elongated spermatids were found in seminiferous tubules. Blue arrows indicate spermatocytes and meiotic phase. Blue arrowheads indicate round spermatids (scale bar 25 μm). (F and G) HE staining of epididymis from *RanBP1*$^{+/+}$ (F) and *RanBP1*$^{-/-}$ (G) mice (scale bar 100 μm).

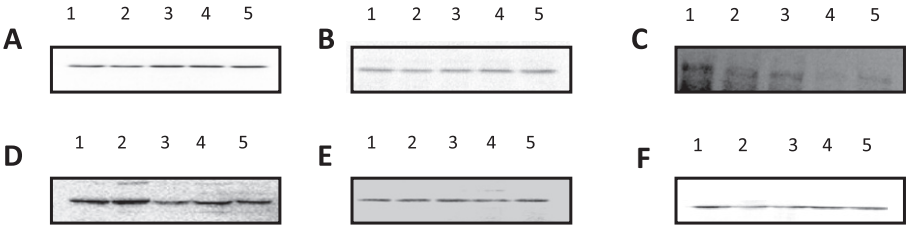

Fig. 4. Expression patterns of RanGTPase cycle regulators during mouse spermatogenesis. Lanes 1–5 are testis lysate samples from WT mice of 1–5 weeks of age, respectively. Ran, (B) RanBP1, (C) RanBP2, (D) RanGAP, (E) RCC1, (F) actin (a loading control).

~30 genes exist in the region, a gene that can account for the wide range of DGS symptoms has not yet been identified [24]. Although no case of a male DGS patient who exhibited infertility has been reported, it may be meaningful to determine whether some DGS patients display infertility owing to a mutation(s) in the other allele of the *RanBP1* gene. Intriguingly, some DGS patients have been clinically reported to show growth retardation [25], reminiscent of the small body size observed in the RanBP1-knockout mice. Thus, the growth retardation symptom of DGS may be explained by the reduced expression of RanBP1.

On the other hand, it has recently been reported that cultured peripheral sensory neurons respond to axon injury by locally regulating the RanGTPase cycle [9], raising the possibility that RanBP1-knockout mice may show some neuronal defects just after injury.

Finally, recent studies have reported that siRNA-mediated depletion of RanBP1 alone leads to significant cell death in some cancer cell lines (HeLa, U2OS) [19,20]. Intriguingly, microarray analyses have revealed that RanBP1 is overexpressed in various tumor specimens, such as squamous lung carcinoma and esophageal carcinoma [3]. These observations also suggest that RanBP1 plays some roles independent of RanBP2 at least in some cancer cells. RanBP1-knockout mice will be of use to elucidate the entire complement of RanBP1 functions.

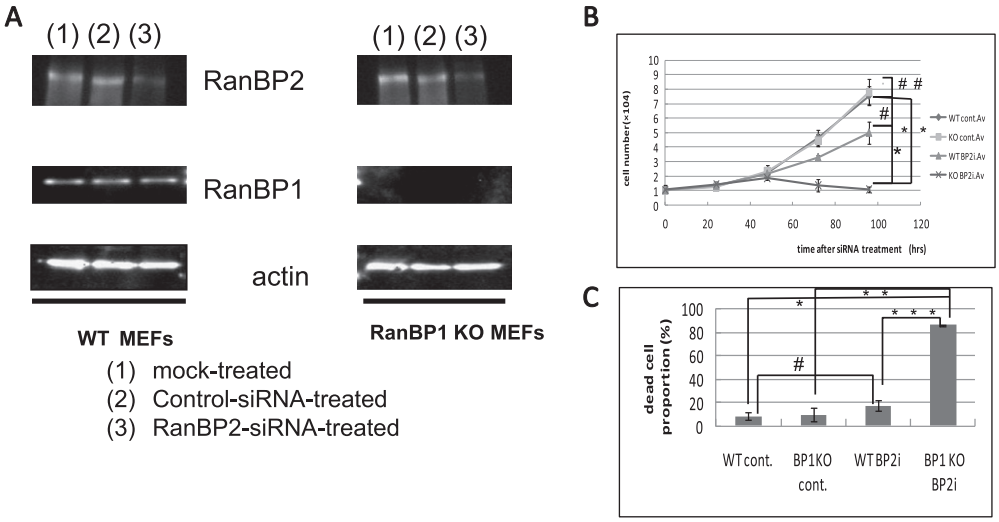

Fig. 5. *RanBP1*$^{-/-}$ MEFs proliferate normally and siRNA-mediated RanBP2-depletion causes severe damage specifically in *RanBP1*$^{-/-}$ MEFs. (A) Confirmation of RanBP2-depletion in RanBP2-siRNA-treated MEFs by immunoblot analysis ((1) mock (2) control-siRNA-treated (3) RanBP2-siRNA-treated). (B) Growth curves of WT and *RanBP1*$^{-/-}$ MEFs (Passage 3) treated with control- or RanBP2-siRNA for 4 days after siRNA transfection ($^{*}P = 7.52 \times 10^{-3}$; $^{**}P = 2.40 \times 10^{-4}$; $^{\#}P = 7.93 \times 10^{-3}$; $^{\#\#}P = 0.722$). (C) Cellular viability determination by trypan-blue staining ($^{*}P = 5.05 \times 10^{-6}$; $^{**}P = 2.87 \times 10^{-5}$; $^{***}P = 1.36 \times 10^{-5}$; $^{\#}P = 0.0431$).

Acknowledgements

We are grateful to Mattaj, I. W., Nagata, S., Weis, K., Jans, D. A., Loveland, K. L., Miyamoto, Y., Hieda, M., Nagai, Y., Yamamoto, M., Shima, Y., Morimoto, K., Fujiwara, T. and all the members of Biomolecular Dynamics group members for helpful discussions. We deeply thank Takeda, J., Ijiri, T. for providing pMulti-ND-1.0 vector, Kawai, A. for generating chimeric mice, and Muraoka, R., Okamura, M. for secretarial assistance. This work was supported by the Japanese Ministry of Education, Culture, Sports, Science and Technology, the Japan Society for the Promotion of Science, and the Takeda Science Foundation.

Appendix A. Supplementary data

Supplementary data associated with this article can be found, in the online version, at doi:10.1016/j.febslet.2011.02.002.

References

[1] Bischoff, F.R. and Ponstingl, H. (1991) Catalysis of guanine nucleotide exchange on Ran by the mitotic regulator RCC1. Nature 354, 80–82.
[2] Clarke, P.R. and Zhang, C. (2008) Spatial and temporal coordination of mitosis by Ran GTPase. Nat. Rev. Mol. Cell Biol. 9, 464–477.
[3] Di Fiore, B., Ciciarello, M. and Lavia, P. (2004) Mitotic functions of the Ran GTPase network: the importance of being in the right place at the right time. Cell Cycle 3, 305–313.
[4] Weis, K. (2003) Regulating access to the genome: nucleocytoplasmic transport throughout the cell cycle. Cell 112, 441–451.
[5] Hetzer, M., Gruss, O.J. and Mattaj, I.W. (2002) The Ran GTPase as a marker of chromosome position in spindle formation and nuclear envelope assembly. Nat. Cell Biol. 7, E177–E184.
[6] Dasso, M. (2002) The Ran GTPase: theme and variations. Curr. Biol. 12, R502–R508.
[7] Yoneda, Y. (2000) Nucleocytoplasmic protein traffic and its significance to cell function. Genes Cells. 5, 777–787.
[8] Gorlich, D. and Kutay, U. (1999) Transport between the cell nucleus and the cytoplasm. Annu. Rev. Cell. Dev. Biol. 15, 607–660.
[9] Yudin, D., Hanz, S., Yoo, S., Iavnilovitch, E., Willis, D., Gradus, T., Vuppalanchi, D., Segal-Ruder, Y., Ben-Yaakov, K., Hieda, M., Yoneda, Y., Twiss, J.L. and Fainzilber, M. (2008) Localized regulation of axonal RanGTPase controls retrograde injury signaling in peripheral nerve. Neuron 59, 241–252.
[10] Bischoff, F.R., Krebber, H., Kempf, T., Hermes, I. and Ponstingl, H. (1995) Human RanGTPase-activating protein RanGAP1 is a homologue of yeast Rna1p involved in mRNA processing and transport. Proc. Natl. Acad. Sci. USA 92, 1749–1753.
[11] Coutavas, E., Ren, M., Oppenheim, J.D., D'Eustachio, P. and Rush, M.G. (1993) Characterization of proteins that interact with the cell-cycle regulatory protein Ran/TC4. Nature 366, 585–587.
[12] Bischoff, F.R., Krebber, H., Smirnova, E., Dong, W. and Ponstingl, H. (1995) Co-activation of RanGTPase and inhibition of GTP dissociation by Ran-GTP binding protein RanBP1. EMBO J. 14, 705–715.
[13] Bischoff, F.R. and Gorlich, D. (1997) RanBP1 is crucial for the release of RanGTP from importin beta-related nuclear transport factors. FEBS Lett. 419, 249–254.
[14] Schlenstedt, G., Wong, D.H., Koepp, D.M. and Silver, P.A. (1995) Mutants in a yeast Ran binding protein are defective in nuclear transport. EMBO J. 14, 5367–5378.
[15] Oupenski, I.I., Mueller, U.W., Matynia, A., Sazer, S., Elledge, S.J. and Brinkley, B.R. (1995) Ran-binding protein-1 is an essential component of the Ran/RCC1 molecular switch system in budding yeast. J. Biol. Chem. 270, 1975–1978.
[16] Yokoyama, N., Hayashi, N., Seki, T., Panté, N., Ohba, T., Nishii, K., Kuma, K., Hayashida, T., Miyata, T., Aebi, U., Fukui, M. and Nishimoto, T. (1993) A giant nucleopore protein that binds Ran/TC4. Nature 376, 184–188.
[17] Aslanukov, A., Bhowmick, R., Guruju, M., Oswald, J., Raz, D., Bush, R.A., Sieving, P.A., Lu, X., Bock, C.B. and Ferreira, P.A. (2006) RanBP2 modulates Cox11 and hexokinase I activities and haploinsufficiency of RanBP2 causes deficits in glucose metabolism. Plos Genet., e17.
[18] Dawlaty, M.M., Malureanu, L., Jeganathan, K.B., Kao, E., Sustmann, C., Tahk, S., Shuai, K., Grosschedl, R. and van Deursen, J.M. (2008) Resolution of sister centromeres requires RanBP2-mediated SUMOylation of topoisomerase IIalpha. Cell 133, 103–115.
[19] Li, H.Y., Ng, W.P., Wong, C.H., Iqulesias, P.A. and Zheng, Y. (2007) Coordination of chromosome alignment and mitotic progression by the chromosome-based Ran signal. Cell Cycle 6, 1886–1895.
[20] Tedeschi, A., Ciciarello, M., Mangiacasale, R., Roscioli, E., Rensen, W.M. and Lavia, P. (2007) RANBP1 localizes a subset of mitotic regulatory factors on spindle microtubules and regulates chromosome segregation in human cells. J. Cell. Sci. 120, 3748–3761.
[21] Hogarth, C., Itman, C., Jans, D.A. and Loveland, K.L. (2005) Regulated nucleocytoplasmic transport in spermatogenesis: a driver of cellular differentiation? Bioessays 10, 1011–1025.
[22] Tanaka, H. and Baba, T. (2005) Gene expression in spermiogenesis. Cell. Mol. Life Sci. 62, 344–354.
[23] Tokuhiro, K., Hirose, M., Miyagawa, Y., Tsujimura, A., Irie, S., Isotani, A., Okabe, M., Toyama, Y., Ito, C., Toshimori, K., Takeda, K., Oshio, S., Tainaka, H., Wada, M., Tsuchida, J., Okuyama, A., Nishimune, Y. and Tanaka, H. (2008) Meichroacidin containing the membrane occupation and recognition nexus motif is essential for spermatozoa morphogenesis. J. Biol. Chem. 283, 19039–19048.
[24] Lindsay, E.A. (2001) Chromosomal microdeletions: dissecting del22q11 syndrome. Nat. Rev. Genet., 2858–2868.
[25] Ryan, A. K., Goodship, J.A., Wilson, D.I., Philip, N., Levy, A., Seidel, H., Schuffenhauer, S., Oechsler, Belohradsky, B., Prieur, M., Aurias, A., Raymond, F. L., Clayton-Smith, J., Hatchwell, E., McKeown, C., Beemer, F. A., Dallapiccola, B., Novelli, G., Hurst, J. A., Ignatius, J., Green, A. J., Winter, R. M., Brueton, L., Brøndum-Nielsen, K., and Scambler, P. J. (1997) Spectrum of clinical features associated with interstitial chromosome 22q11 deletions: a European collaborative study. J. Med. Genet. 34, 798–804.